LARP1 binding to hepatitis C virus particles is correlated with intracellular retention of viral infectivity

Authors:

Marie-Laure Plissonnier[1#], Jessica Cottarel[1#], Eric Piver[2], Majlinda Kullolli[3], Federica Grazia Centonze[4], Sharon Pitteri[3], Hesso Farhan[4], Jean-Christophe Meunier[2], Fabien Zoulim[1,6], Romain Parent[1*]

Co-first authors

Affiliations:

[1] Pathogenesis of Hepatitis B and C - DEVweCAN LabEx, INSERM U1052-CNRS 5286, Centre de Recherche en Cancérologie de Lyon, Université de Lyon, F-69008 Lyon, France

[2] Morphogenesis and antigenicity of HIV and hepatitis viruses, INSERM U966, Université de Tours, F-37000 Tours, France.

[3] Canary Center for Cancer Early Detection, Department of Radiology, Stanford University School of Medicine, Palo Alto, CA 94304, USA

[4] Institute of Basic Medical Science, University of Oslo, N-0372 Olso, Norway

[6] Lyon University Hospital (Hospices civils de Lyon), Hepatogastroenterology Service, F-69001 Lyon, France

***Corresponding author:** Romain Parent, E-mail: romain.parent@inserm.fr, Phone: +00 33 4 72 68 19 70, Fax: +00 33 4 72 68 19 71. Mailing address: Inserm U1052, 151 Cours Albert Thomas, F-69424 Lyon Cedex 03, France.

Conflict of interest statement: None

Manuscript type: research article

Word count: 147 (summary); 4486 (main text)

Number of figures: 6

Number of supplementary figures: 1

Funding sources

This work was funded by the EU Marie Curie International Reintegration Program (IRG#248364 to RP), the Lyric Grant INCa-DGOS-4664 (FZ, RP) and the ANRS (#2011-031) for RP. MLP and JC are recipients of ANRS and Lyric post-doctoral fellowships, respectively. Funding sources had no role in study design, in the collection, analysis and interpretation of data, in the writing of the report, and in the decision to submit the article for publication.

Abstract

Hepatitis C virus (HCV) virions contain a subset of host liver cells proteome often composed of interesting virus-interacting factors. A proteomic analysis performed on double gradient-purified clinical HCV highlighted the translation regulator LARP1 on these virions. This finding was validated using post-virion capture and immunoelectron

microscopy, immunoprecipitation applied to *in vitro* (Huh7.5 liver cells) grown (Gt2a, JFH1 strain) and patient-derived (Gt1a) HCV particles. Upon HCV infection of Huh7.5 cells, we observed a drastic transfer of LARP1 to lipid droplets, inducing colocalization with core proteins. RNAi-mediated depletion of LARP1 using the C911 control approach decreased extracellular infectivity of HCV Gt1a (H77), Gt2a (JFH1), and Gt3a (S52 chimeric strain), yet increased their intracellular infectivity. This latter effect was unrelated to changes in the hepatocyte secretory pathway, as evidenced using a functional RUSH assay. These results indicate that LARP1 binds to HCV, an event associated with retention of intracellular infectivity.

Keywords

LARP1, HCV, infectivity, virions

Introduction

Viruses and primate cells have coexisted for several million years. Host cells have evolved to eliminate most replicating viruses according to paleovirology studies (Patel et al., 2011). Therefore virion-bound host proteins (VBPs) may be considered to provide viral species with important components for virus persistence and/or propagation through their implication in replication, egress or entry steps of the viral cycle (Arthur et al., 1992; Garrus et al., 2001). Assuming that VBPs are likely to play a more important role in the viral life cycle than the rest of the cell proteome, the aim of our study was to validate the presence of some VBPs on hepatitis C virus (HCV) virions and to unravel a potential role for these VBPs at the entry or egress levels.

HCV is an enveloped positive-strand RNA virus and belongs to the genus *Hepacivirus* in the *Flaviviridae* family. HCV often establishes persistent infection in humans, which may lead to chronic liver disease, cirrhosis, and hepatocellular carcinoma, the third most common cause of cancer-related death (El-Serag, 2012). HCV infects hepatocytes and induces extensive remodeling of endoplasmic reticulum (ER)-derived membranes into a so-called "membranous web" (Egger et al., 2002). This web is composed of double membrane vesicles located in close proximity to lipid droplets (LDs) and serves as the site of viral genome replication and particle assembly (Aizaki et al., 2004), prior to release via the secretory pathway, though the precise mechanisms underlying this export process are not fully understood.

HCV comprises both an abundant amount and a broad variety of VBPs. Indeed, HCV virions incorporate not only viral but also host proteins, many of which, notably apolipoproteins B and E, have been shown to be functionally implicated in the viral life cycle by modulating cellular processes involved in lipid metabolism (Chang et al., 2007) (Huang et al., 2007; Meunier et al., 2008). In addition, HCV VBPs implicated in

protein folding, e.g. HSC70 (Parent et al., 2009), as well as others functions (Benga et al., 2010; Cottarel et al., 2016) have been identified.

The La-Related Protein 1 (LARP1) is a highly evolutionarily conserved translation regulating and RNA-binding protein (RBP) of the LARP family, each member of which carries a conserved La domain and an RNA-binding region. Following a recent upsurge in studies focusing on LARP1 in human biology, after its initial investigation in plants (Merret et al., 2013), this RBP was identified as a regulator of both mRNA stability and translation (Gentilella et al., 2017; Hong et al., 2017; Lahr et al., 2017), especially with respect to transcripts implicated in cell proliferation and cell survival (Stavraka and Blagden, 2015). Interestingly, LARP1 is overexpressed in hepatocellular, lung and ovarian cancers, where it is an independent predictor of adverse prognosis (Xie et al., 2013) (Hopkins et al., 2016). Moreover, the level of LARP1 is elevated in squamous cervical cancer, where it promotes cell motility and invasion, and binds an mRNA interactome enriched in oncogenic transcripts (Mura et al., 2015). In this study, we identify LARP1 as a novel component of at least a subset of HCV particles and show that it plays a role in the virus life cycle, predominantly by restricting the release of three epidemiologically important HCV genotypes.

Results

In order to identify host cell factors that associate with circulating HCV virions, we performed a proteomic analysis of HCV particles isolated from the plasma of two viremic patients. Plasma from an aviremic subject served as a control. After initial pelleting, HCV particles were sedimented on two sequential iodixanol gradients via isopycnic centrifugation as described previously (Cottarel et al., 2016; Parent et al., 2009). By monitoring HCV RNA in the collected fractions, we identified a peak of viral

RNA at 1.12 g/mL of iodixanol (Fig. 1). To further decrease the level of non-specific co-sedimented background material, we subjected our virus-containing fractions to a second iodixanol gradient-based purification step, together with a naïve plasma sample (Parent et al., 2009). Following HPLC/MS analysis of the virus-containing fractions as described before (Cottarel et al., 2016) (Parent et al., 2009), we detected LARP1 in these fractions, but not in the corresponding aviremic control.

In order to confirm the presence of LARP1 on the particles, we immunoprecipitated LARP1 from JFH1 virus released from Gt2a HCVcc-infected Huh7.5 cells (Delgrange et al., 2007) with anti-LARP1 or anti-HCV E2 (CBH5) (Keck et al., 2005). Material was then subjected to silica beads-based RNA extraction and RT-qPCR using HCV primers. As expected, our positive control, the human anti-E2 CBH5 monoclonal antibody displayed the highest enrichment ratio (8-fold) when compared to an isotype control. RNA of *in vitro* produced HCV could be enriched 4-fold using an anti-LARP1 Ig compared to its isotypic control (Fig. 2a). Delipidated particles using NP40 (0.1%, 4°C, overnight) did not immunoprecipitate (not shown) using anti-LARP1 antibodies, suggesting that LARP1 associates with HCV externally rather than being encapsidated.

To seek further evidence that LARP1 is associated with HCV virions, we performed immunogold electron microscopy (IEM) on supernatants of infected Huh7.5 cells, and also used immunocapture (Piver et al., 2017) as an alternative and independent EM-related approach. Viral suspensions were generated from the supernatants of JFH1-infected Huh7.5 cells which were clarified and concentrated on sucrose cushions (Parent et al., 2009) or from patient plasma as previously described (Piver et al., 2017). Suspensions were adsorbed on grids and processed (Cottarel et al., 2016). As shown in Fig. 2b (left set of images), no virion-like structure was observed in HCV-negative

supernatants. No labeling was found for HCV-positive samples stained with secondary antibodies only, ruling out non-specific staining. Although labeling was scarce, an issue commonly encountered in IEM, as illustrated by our previous ApoE staining (Cottarel et al., 2016; Parent et al., 2009), probing HCV-positive supernatants with anti-LARP1 antibodies exposed virions of 30-60 nm in size (Fig. 2b, right set of images), corroborating previously published features of *in vitro*-derived viral particle preparations (Catanese et al., 2013). Gold particles located ≤ 40 nm (corresponding to a single immunoglobulin length) away from the virion were considered to be specifically bound. These data were confirmed using our recently developed immunocapture approach (Piver et al., 2017), implemented here based on anti-E2 and anti-LARP1 antibodies, and which also revealed small-sized virions (Fig. 2c).

Virion-bound host proteins often contribute to viral budding, not least due to their specific intracellular localization, as initially highlighted in the HIV field (Garrus et al., 2001). Using confocal immunofluorescence microscopy, we studied the localization of LARP1 with respect to the infection status of Huh7.5 cells and vicinity of LDs as major sites for HCV morphogenesis (Miyanari et al., 2007), followed by the investigation of several HCV parameters. LARP1 produced a diffuse signal in the cytosol of uninfected cells, while it relocated to the immediate proximity of LDs upon infection, in most cases exhibiting near total colocalization with the typical LD-associated HCV core protein (Fig. 3a). These data were quantitatively verified using Pearson, morphometric and Li correlation coefficient approaches (Fig. 3b-d). Despite several attempts, co-immunoprecipitation assays between HCV core and LARP1 remained unsuccessful, suggesting a labile interaction between both proteins at this level. These results indicate that an important fraction of the LARP1 cytosolic pool accumulates around core-decorated ER/LD structures as previously documented (Miyanari et al., 2007) in

an HCV-positive cell-specific manner. No concomitant increase in LARP1 levels upon infection could be consistently observed (Suppl. Fig. 1). Altogether such data argue for a role for LARP1 in viral assembly processes.

To test this hypothesis, we then modulated LARP1 expression and tested its effect on HCV replication and infectivity. LARP1 levels were transiently modulated by the infection. Huh7.5 cells were transfected with non targeting siRNAs, LARP1 C911-mutated LARP1 siRNAs (Buehler et al., 2012) as a control for excluding off-target effects, or with wt LARP1 siRNAs. Knockdown efficiency was verified by RT-qPCR and Western blotting (Fig. 4a,b). LARP1 depletion-mediated toxicity was ruled out after performing Sulforhodamine B (SRB) (Vichai and Kirtikara, 2006) and Neutral Red (NR) (Repetto et al., 2008) assays (Fig. 4c,d).

The virological consequences of LARP1 depletion were then addressed, by initially considering the highly propagative HCV JFH1 (Gt2a) strain. As shown in Fig. 5a,b, LARP1 depletion weakly decreased (< 2-fold) intracellular HCV RNA Gt2a levels, though no effect was detected extracellularly. This depletion was correlated with a strong increase in intracellular infectivity (up to 3.5-fold, see Materials and methods section) (Fig. 5c). Intriguingly, no significant effect could be observed on extracellular infectivity (Fig. 5d). The same approach was implemented to determine relative infectivity levels, by measuring $TCID_{50}$/HCV RNA ratios, thus evaluating the intracellular RNA-to-particle conversion yield. Similarly to global infectivity levels, RNAi depletion of LARP1 increased the relative intracellular infectivity up to 3-fold (Fig. 5e). Interestingly, a weak (< 2-fold) reduction in the relative extracellular (particle to RNA copies) infectivity levels could be observed (Fig. 5f), which were confirmed through secreted HCV core antigen (Ag) levels (Fig. 5g).

Finally, we evaluated the validity of these results across other HCV genotypes. We therefore tested the consequences of LARP1 depletion on the H77 (Gt1a) (Blight et al., 2003; Yanagi et al., 1997) and Gt3a-bearing S52 chimeric (Gottwein et al., 2011a) strains after electroporation. Post-electroporation viability and proliferative capacity of the cells were similar in all instances (Fig. 6a-b-e-f). While no difference could be observed at the HCV RNA level irrespective of LARP1 conditions (Fig 6c-g), significant inhibition (> 2-fold and 10-fold for Gt1a and Gt3a, respectively) of secreted HCV core Ag levels was observed upon LARP1 depletion (Fig. 6d-h). Lack of HCV RNA reduction following siRNA transfection was probably due to the presence in excess of *in vitro* transcribed RNA copies, while absence of detection of intracellular infectivity reflects the poor, if any, propagation rate of non JFH1 strains in vitro. Nevertheless, these findings suggest trans-genotypic validity of our results.

To verify whether the enhancing impact of LARP1 depletion on HCV intracellular infectivity was due to its general impact on the secretory pathway of the hepatocyte, we conducted a RUSH (retention using selective hooks) assay (Boncompain and Perez, 2013). Since LARP1 depletion did not impair the trafficking of secretory cargoes between the ER and the Golgi apparatus (Suppl. Fig. 2), i.e. increased infectivity was not due to increased viral output, we postulate that LARP1 is involved in restricting viral infectivity downstream of the replication phase. These results may also indicate that the enhanced intracellular infectivity occasioned by LARP1 depletion is reversed and/or compensated by other structural components during the secretory process prior to the extracellular particle release.

Discussion

A virus may contain host proteins for the following reasons: the host protein is present at the site of assembly, the protein interacts with a viral protein and is swept up into the virion during budding, or its incorporation is needed to perform a specific function for the virus. Taken together, derived from MS as well as two methodologically-unrelated approaches, our data identify LARP1 as a component of at least a subset of *in vitro*-grown (Gt2a) and clinical (Gt1a) HCV virions. These data also suggest that some LARP1 regions are exposed on the surface of the secreted viral particle since the protein is accessible for antibody binding, though the mechanisms underlying this exposure should be further ascertained. Indeed, HCV buds through the ER membrane and it is therefore expected that virion-bound proteins such as LARP1 that are accessible to antibody binding in IP/RT-qPCR and $TCID_{50}$ assays translocate to the ER lumen prior to their association with the virion. LARP1 rapidly colocalizes with the peri-droplet HCV core signals but not with the envelope E2 glycoprotein. The association of LARP1 with nascent virions may therefore consist in its intercalation either (i) between the ER-derived membrane and the capsid or (ii) as a virion membrane embedded protein. Since none of the LARP1 primary sequence features encode for a signal peptide, as evidenced by its analysis using Predisi or SignalP 4.0 (Petersen et al., 2011) software, non-canonical translocation processes (Giuliani et al., 2011; Nickel and Rabouille, 2009; Nickel and Seedorf, 2008) may thus arise.

These antibody-based results finally indicate that LARP1 plays a role in early interactions of at least a subset of particles with their target cells, as observed for other VBPs (Chang et al., 2007) (Parent et al., 2009). Since HCV displays a high level of association with non viral-encoded host material (Chang et al., 2007) (Huang et al., 2007; Meunier et al., 2008), and, in this study, LARP1 inferring intracellular retention

of infectivity across three genotypes, this implies that such material must therefore be of specific structural importance for the life cycle of this pathogen (Lavie and Dubuisson, 2017).

LARP1 was characterized relatively recently and has proven of interest in the field of the Dengue virus (Suzuki et al., 2016), another *Flaviviridae* member. LARP1 is overexpressed in HCC and that it is associated with poorer prognosis (Xie et al., 2013). While our study specifically focused on basic virology of HCV, it may prove pertinent to consider a potential association between intrahepatic LARP1 levels and HCV levels at the cirrhotic stage, the most exposed condition for HCC onset in patients. The fact that LARP1 may restrict HCV propagation deserves further investigation in light of its HCC-related protein status and the decreased viremia observed in HCC in the clinic (Reid et al., 1999).

Author statement

MLP conceived and implemented experiments, analyzed the data and wrote the paper. JC, EP, MK, SP, HF, JCM and RP conceived and implemented experiments as well as analyzed the data. FZ co-obtained funding and edited the paper. RP obtained funding and wrote the paper.

Funding information

This work has been funded by the EU Marie Curie International Reintegration Program (#248364 to RP), the Lyric Grant INCa-DGOS-4664 (FZ, RP) and the ANRS (#2011-031) to RP. MLP and JC were recipients of ANRS and Lyric post-doctoral fellowships, respectively.

Acknowledgements

We thank T. Wakita (U. of Tokyo, Japan) and C. Wychowski (CNRS, Lille, France) for the gift of the JFH1 adapted strain, J. Bukh (U. of Copenhagen, Denmark) for the gift of the S52 chimeric strain as well as C.M. Rice (Rockefeller U. NY, USA) for the gift of Huh7.5 cells and the H77 strain. We also thank E. Errazuriz-Cerda, A. Bouchardon (Ciqle, U. of Lyon, France) for confocal and electron microscopy. We are indebted to B. Bartosch and CA. Eberle (Inserm, France) for discussion.

Conflict of interest statement

We have no conflict of interest to declare.

Ethical statement

The study complies with the COPE guidelines. Patient samples were obtained and processed after approval of the French IRB (CPP South-East II, agreement #2010-08-AM2).

Materials and methods

Purification of HCV virions

Infected plasma was obtained from three HCV-positive patients and an aviremic control and processed after approval of the French IRB (CPP South-East II, agreement #2010-08-AM2). Plasmas were stabilized with 10 mM Hepes (Gibco), antiproteases (Roche), centrifuged at 8,000 g for 15 min at 4°C, filtered through 0.45 µm membranes, layered onto a 20% sucrose cushion in TNE (10 mM Tris, 150 mM NaCl, 2 mM EDTA) and ultracentrifuged at 27,000 rpm for 4 h at 4°C. Pellets were then resuspended in 1 mL of TNE, layered on top of 15-40% iodixanol gradients, and submitted to isopycnic

ultracentrifugation for 16 h at 31,200 rpm at 4°C. Fractions were then harvested from the top of the gradient. The amount of HCV RNA in each fraction was determined by real-time quantitative polymerase chain reaction (RT-qPCR). The fractions with the highest RNA content and the corresponding fractions from the uninfected control were pooled and dialyzed against TNE overnight at 4°C. Fractions were then concentrated 10- to 20-fold in YM-3 concentration devices (Centricon; Millipore, Billerica, MA), subjected to a second ultracentrifugation step as described above and processed for mass spectrometry.

Electron microscopy

Viral suspensions were generated from infected cell supernatants or patient plasma which was clarified and then concentrated on a 20% sucrose cushion as described (Parent et al., 2009). Suspensions were adsorbed on 200 mesh Nickel grids coated with formvar-C for 2 min at room temperature (RT). Immunogold labeling was performed by floating the grids on droplets of reactive medium. Grids were blocked in 1% BSA / 1% normal goat serum / 50 mM Tris-HCl, pH 7.4 for 10 min at RT. Incubation with anti-LARP1 primary antibodies (40 µg/ml) was carried out in a wet chamber for 2 h at RT. Following successive washes in 50 mM Tris-HCl, pH 7.4 and pH 8.2 at RT, grids were first incubated in 1% BSA / 50 mM Tris-HCl, pH 8.2 in a wet chamber for 10 min at RT and then labeled with 10 nm gold-conjugated IgG (Aurion) diluted 1/80 in 1% BSA / 50 mM Tris-HCl pH 8.2 for 45 min. Grids were then subjected to two washes in 50 mM Tris-HCl pH 8.2 and pH 7.4 and finally rinsed in distilled water. Following a 2 min fixation with 4% glutaraldehyde, grids were stained with 2% phosphotungstic acid for 2 min and then analyzed using a transmission electron microscope (Jeol 1400 JEM, Tokyo, Japan) equipped with a Gatan camera (Orius 600) and a Digital

Micrograph Software.

Immunocapture

The formvar-carbon EM grids (S162, Oxford Instruments) were initially incubated with 0.01% poly-L lysine for 30 min at RT and then with selected antibodies (20 µg/mL) for 1 h at RT. Grids were washed in PBS and incubated with biological samples containing or not viral particles, for 2 h at RT. EM grids were washed in PBS and incubated for 20 min in 4% paraformaldehyde and 1% glutaraldehyde in 0.1 M phosphate buffer, pH 7.2. Particles trapped on grids were stained with 0.5% uranyl acetate for examination under a JEOL 1230 transmission electron microscope (Piver et al., 2017).

Cell culture and HCV infection / electroporation.

The human hepatoma cell line Huh7.5 was cultured in Dulbecco's minimal essential medium (DMEM; Life Technologies) supplemented with 10% fetal bovine serum (FBS; Thermo Scientific) and 1% penicillin-streptomycin (Life Technologies). Viral stocks (Gt2a) or experiments (Gt1a and Gt3a) were generated via transfection of *in vitro* transcripts encoding the JFH1 genotype 2a-derived strain (Delgrange et al., 2007) or H77 (Yanagi et al., 1997) and S52 (Gottwein et al., 2010; Gottwein et al., 2011b) strains. $2x10^4$ cells/cm^2 were infected with HCV JFH1 at an MOI of 0.1.

siRNA-mediated knockdown

Twenty thousand cells per square centimeter were transfected with 33 nM final concentration of non-targeting control siRNAs, C911-mutated LARP1 siRNAs (Buehler et al., 2012) or wt LARP1 siRNAs (Sigma-Aldrich, sense strand, 5'-3': GGUGACUUUGGAGAUGCAAUC, antisense strand, 5'-3':

GAUUGCAUCUCCAAAGUCACC) using Lipofectamine 2000 (Invitrogen), according to the manufacturer's instructions. The target sequence of LARP1, 5'-3': GGTGACTTTGGAGATGCAATC corresponds to the GenBank Acc.# NM_015315.

Immunofluorescence

siRNA-transfected Huh7.5 cells were fixed in 2% paraformaldehyde, permeabilized and blocked with 0.1% triton X-100 / 3% BSA in PBS at RT, then stained with the primary antibodies overnight at 4°C (anti-LARP1 from Novus #NBP1-19128, anti-HCV core clone #C7/50 from Santa Cruz, 2 µg/mL) and finally incubated with Alexa–conjugated secondary antibodies (1 µg/mL). Cell nuclei were counterstained with Hoechst 33358 (0.025µg/mL in PBS) and visualized under a Leica SP5 confocal microscope. Overlaid images were obtained using the ImageJ software.

Immunoblotting

Immunoblotting was performed using 30 µg of RIPA-resuspended Huh7.5 cell lysates, then resolved on 10% SDS-PAGE, blotted onto nitrocellulose membranes (Amersham Biosciences), blocked using 5% low fat dried milk in PBS for 1hr at RT and probed overnight at 4°C with antibodies raised against LARP1 (1/1,000; Novus Biologicals, cat. #NBP1-19128) and tubulin (1/10,000; Sigma-Aldrich, cat. #T5168).

Immunoprecipitation and neutralization assays

Supernatants from infected cells were harvested 4 days post infection, cleared by centrifugation (8,000 g, 15 min. 4°C) and then supplemented with 10 mM HEPES and protease inhibitors. Immunoprecipitation of secreted virions with antibodies coupled to protein G magnetic beads (Pierce, 2 µg/IP) was carried out as described previously

(Jammart et al., 2013). Material was then subjected to RNA extraction (Qiagen) and RT-qPCR.

HCV $TCID_{50}$ infectivity assay

Cells were seeded onto 96-well plates (6,400 cells/well) the day before infection. Cells were then inoculated with 10-fold serial dilutions of the supernatants of interest. 96 h post-infection, cells were washed in PBS, fixed for 10 min in methanol/acetone and blocked for 30 min in 1X PBS / 5% BSA at RT. Cells were then probed with in-house HCV antiserum (#1804; 1/500) in 1X PBS / 3% BSA for 1hr at RT. After three washes in 1X PBS / 3% BSA, bound primary antibodies were probed with 1 µg/mL goat anti-human Alexa Fluor 488 secondary antibodies (Life Technologies) for 1hr at RT and visualized by epifluorescence (Nikon TE2000E). Viral titers were determined using the adapted Reed & Münch method (Lindenbach, 2009).

Neutral Red assay

The Neutral Red (NR) assay was conducted as described by Repetto (Repetto et al., 2008). Briefly, the NR stock solution (40 mg NR dye in 10 mL PBS) was diluted in culture medium to a final concentration of 4 mg/mL and then centrifuged at 600 g for 10 min to remove any precipitated dye crystals. Cells were then incubated with 100 µL of NR medium for 1hr. NR medium was removed and the cells washed with PBS. Plates were incubated for 10 min under shaking with 150 µL/well of NR destain solution (50% ethanol 96%, 49% deionized water, 1% glacial acetic acid). OD was measured at 540 nm in a microplate spectrophotometer.

Sulforhodamine B assay

Cells were incubated with 100 µL of 0.057% Sulforhodamine B (SRB) at RT for 30 min and then rinsed four times with 1% acetic acid, followed by four washes with distilled water. Plates were left to dry at RT and then incubated in 200 µL of 10 mM Tris pH 10.5. Plates were placed on an orbital shaker for 5 min and OD measured at 510 nm in a microplate reader.

Quantitative RT-PCR

Total RNA was extracted using trizol (Invitrogen). 1 µg of RNA was DNAse I-digested (Promega) and then reverse transcribed using MMLV reverse transcriptase (Invitrogen) according to the manufacturer's instructions. Quantitative real-time PCR was performed on a LightCycler 480 device (Roche) using the iQ SYBR Green Supermix (Bio-Rad). PCR primers sequences (5'-3') and qPCR conditions were defined as follows: GUS-F: CGTGGTTGGAGAGCTCATTTGGAA, GUS-R: ATTCCCCAGCACTCTCGTCGGT, HCV RC1: GTCTAGCCATGGCGTTAGTA, HCV RC21: CTCCCGGGGCACTCGCAAGC, LARP1-F: TCAAACTTTCGGTAGCCAAACT, and LARP1-R: GCCTGGCAACCAGAGATCAAA. Annealing temparature was 55°C in all instances. Primer specificity was assessed by melting curves and agarose gel electrophoresis.

HCV core Elisa assay

The supernatants (100 µl) of HCV Gt1a-, Gt2a- and Gt3a-infected cells were spun down (8,000 g, 5 min, 4°C) prior to Elisa processing using the Quick titer HCV core Antigen Elisa kit (Cell Biolabs Inc) according to the manufacturer's instructions.

Figure legends

Figure 1. Double gradient-based enrichment of HCV particles harvested from clinical material.

Clarified and 20% sucrose cushion-pelleted plasmas were subjected to isopycnic fractionation using two sequential 10% to 60% linear iodixanol gradients. HCV RNA levels were determined in each fraction after the first run and fractions bearing the highest viral signal by qPCR were loaded atop the second gradient prior to a second round of qPCR. The density of each fraction was determined using a refractometer. The graph is representative of two independent fractionation processes performed on two distinct patient plasmas. Plasma from an aviremic subject served as co-purification / mass spectrometry negative control and was processed in parallel.

Figure 2. LARP1 is a hepatitis C virus particle-bound host factor.

(a) LARP1-mediated immunoprecipitation of HCV RNA. Supernatants harvested from HCVcc-infected Huh7.5 cells (3 days post-infection (p.i.)) were subjected to clarification and immunoprecipitation using the indicated antibodies. HCV RNA was extracted and subsequently analyzed by RT-qPCR. Mann-Whitney test, $P < 0.05$ (*). (b) Association of LARP1 with cell culture-derived HCVcc evidenced by IEM. Concentrated supernatants of infected Huh7.5 cells were deposited onto EM grids and processed for immunogold labeling using the indicated antibodies. Bound anti-LARP1 antibodies were detected using secondary Igs conjugated to 10 nm gold particles. Pictures are representative of two labeling procedures. (c) Association of LARP1 with cell culture-derived HCV particles evidenced by immunocapture EM. Grids previously coated with control Igs, anti-HCV E2 (clone #AR3A) or anti-LARP1 were then incubated with supernatants of HCV-infected Huh7.5 cells and visualized under TEM. (n = 3 +/- s.d.). Mann-Whitney, $P < 0.05$ (*). For clarity, only highest significance is

shown.

Figure 3. HCV infection triggers LARP1 accumulation around lipid droplets.

(a) LARP1 and core co-localization. HCVcc-infected Huh7.5 cells (3 days p.i.) were fixed, permeabilized and stained for HCV core proteins and LARP1 prior to incubation with Alexa 488 (HCV core signal) and Alexa-594 (LARP1 signal)-conjugated secondary antibodies. Cells were counterstained with Hoechst 33358. Merged images were obtained using the ImageJ software. (b) Pearson co-localization coefficient. Coefficient was calculated using the ImageJ software and plotted against the indicated time points. (c) Morphometric assessment of co-localization. Green (HCV core) and red (LARP1) fluorescence intensities were plotted for each pixel across a representative lipid droplet image as shown (dashed line) using the Plot Profile function of the ImageJ software. Correlation coefficients for the selected couples of intensity values (core/LARP1) are shown. (d) Further statistical assessment of this co-localization dataset implemented using the Li coefficient. Profile of positive staining amplitude values confirm near total co-localization (Bolte and Cordelieres, 2006). Data are representative of six independent experiments.

Figure 4. RNAi-based depletion of LARP1 expression.

(a,b) Cells transfected with siRNAs were subsequently cultured for 24 to 72 h prior to RNA extraction (a) or immunobloting (b). Anti-LARP1-specific primers or anti-LARP1 antibodies, respectively were used. Homogenous loading and blotting were previously assessed by Ponceau Red staining (not shown) and using anti-tubulin antibodies. (c,d) Related cell toxicity assays. The same cultures as **a** were tested for cell proliferation and viability using the SRB and NRA assays, respectively. n = 3, Mann-Whitney test:

ns, non-significant.

Figure 5. Virological consequences of LARP1 depletion.

HCVcc-infected cells were transfected with siRNAs and subsequently cultured for 24 to 72 h prior to: intracellular RNA extraction followed by RT-qPCR using HCV and GUS primers (a), extracellular RNA extraction followed by RT-qPCR using HCV primers (b), intracellular or extracellular $TCID_{50}$ quantification followed by protein normalization (c-d) or by HCV RNA normalization (e-f), and finally (g) secreted HCV core Ag quantification by Elisa (n = 3 +/- s.d.). Mann-Whitney, $P < 0.05$ (*).

Figure 6. Validation of virological consequences of LARP1 depletion in HCV Gt1a and Gt3a (chimeric) strains.

(a-b-e-f). Evaluation of cell viability post-HCV Gt1a (H77) and Gt3a (S52) electroporation using the NRA (a-e) and SRB (b-f) assays. Intracellular RNA extraction followed by RT-qPCR using HCV RC1-RC21 and GUS primers (c-g). Extracellular quantification of secreted HCV core Ag levels (d-h).

Supplementary Figure 1. LARP1 is not modulated by HCV infection.

Cells were infected with HCV at a MOI of 0.1 or left uninfected and cultured for 3 days prior to western blotting using anti-LARP1 and anti-HCV core antibodies. Homogenous loading and blotting were previously assessed by Ponceau Red staining (not shown) and using anti-tubulin antibodies (n = 3).

Supplementary Figure 2. Functionality of the secretory pathway is unaltered by LARP1 depletion.

Huh7.5 cells were transfected with the indicated siRNAs. Co-localization of GM130 and MannII-GFP is shown for each condition at baseline and 20 min post-displacement (n = 2).

References

Aizaki, H., Lee, K.J., Sung, V.M., Ishiko, H., Lai, M.M., 2004. Characterization of the hepatitis C virus RNA replication complex associated with lipid rafts. Virology 324(2), 450-461.

Arthur, L.O., Bess, J.W., Jr., Sowder, R.C., 2nd, Benveniste, R.E., Mann, D.L., Chermann, J.C., Henderson, L.E., 1992. Cellular proteins bound to immunodeficiency viruses: implications for pathogenesis and vaccines. Science 258(5090), 1935-1938.

Benga, W.J., Krieger, S.E., Dimitrova, M., Zeisel, M.B., Parnot, M., Lupberger, J., Hildt, E., Luo, G., McLauchlan, J., Baumert, T.F., Schuster, C., 2010. Apolipoprotein E interacts with hepatitis C virus nonstructural protein 5A and determines assembly of infectious particles. Hepatology 51(1), 43-53.

Blight, K.J., McKeating, J.A., Marcotrigiano, J., Rice, C.M., 2003. Efficient replication of hepatitis C virus genotype 1a RNAs in cell culture. J Virol 77(5), 3181-3190.

Bolte, S., Cordelieres, F.P., 2006. A guided tour into subcellular colocalization analysis in light microscopy. Journal of microscopy 224(Pt 3), 213-232.

Boncompain, G., Perez, F., 2013. Fluorescence-based analysis of trafficking in mammalian cells. Methods in cell biology 118, 179-194.

Buehler, E., Chen, Y.C., Martin, S., 2012. C911: A bench-level control for sequence specific siRNA off-target effects. PloS one 7(12), e51942.

Carlsen, T.H., Pedersen, J., Prentoe, J.C., Giang, E., Keck, Z.Y., Mikkelsen, L.S., Law, M., Foung, S.K., Bukh, J., 2014. Breadth of neutralization and synergy of clinically relevant human monoclonal antibodies against HCV genotypes 1a, 1b, 2a, 2b, 2c, and 3a. Hepatology 60(5), 1551-1562.

Catanese, M.T., Uryu, K., Kopp, M., Edwards, T.J., Andrus, L., Rice, W.J., Silvestry, M., Kuhn, R.J., Rice, C.M., 2013. Ultrastructural analysis of hepatitis C virus particles. Proceedings of the National Academy of Sciences of the United States of America 110(23), 9505-9510.

Chang, K.S., Jiang, J., Cai, Z., Luo, G., 2007. Human apolipoprotein e is required for infectivity and production of hepatitis C virus in cell culture. J Virol 81(24), 13783-13793.

Cottarel, J., Plissonnier, M.L., Kullolli, M., Pitteri, S., Clement, S., Millarte, V., Si-Ahmed, S.N., Farhan, H., Zoulim, F., Parent, R., 2016. FIG4 is a hepatitis C virus particle-bound protein implicated in virion morphogenesis and infectivity with cholesteryl ester modulation potential. J Gen Virol 97(1), 69-81.

Delgrange, D., Pillez, A., Castelain, S., Cocquerel, L., Rouille, Y., Dubuisson, J., Wakita, T., Duverlie, G., Wychowski, C., 2007. Robust production of infectious viral particles in Huh-7 cells by introducing mutations in hepatitis C virus structural proteins. J Gen Virol 88(Pt 9), 2495-2503.

Egger, D., Wolk, B., Gosert, R., Bianchi, L., Blum, H.E., Moradpour, D., Bienz, K., 2002. Expression of hepatitis C virus proteins induces distinct membrane alterations including a candidate viral replication complex. J Virol 76(12), 5974-5984.

El-Serag, H.B., 2012. Epidemiology of viral hepatitis and hepatocellular carcinoma. Gastroenterology 142(6), 1264-1273 e1261.

Garrus, J.E., von Schwedler, U.K., Pornillos, O.W., Morham, S.G., Zavitz, K.H., Wang, H.E., Wettstein, D.A., Stray, K.M., Cote, M., Rich, R.L., Myszka, D.G.,

Sundquist, W.I., 2001. Tsg101 and the vacuolar protein sorting pathway are essential for HIV-1 budding. Cell 107(1), 55-65.

Gentilella, A., Moron-Duran, F.D., Fuentes, P., Zweig-Rocha, G., Riano-Canalias, F., Pelletier, J., Ruiz, M., Turon, G., Castano, J., Tauler, A., Bueno, C., Menendez, P., Kozma, S.C., Thomas, G., 2017. Autogenous Control of 5'TOP mRNA Stability by 40S Ribosomes. Molecular cell 67(1), 55-70 e54.

Giuliani, F., Grieve, A., Rabouille, C., 2011. Unconventional secretion: a stress on GRASP. Curr Opin Cell Biol 23(4), 498-504.

Gottwein, J.M., Jensen, T.B., Mathiesen, C.K., Meuleman, P., Serre, S.B., Lademann, J.B., Ghanem, L., Scheel, T.K., Leroux-Roels, G., Bukh, J., 2011a. Development and application of hepatitis C reporter viruses with genotype 1 to 7 core-nonstructural protein 2 (NS2) expressing fluorescent proteins or luciferase in modified JFH1 NS5A. J Virol 85(17), 8913-8928.

Gottwein, J.M., Scheel, T.K., Callendret, B., Li, Y.P., Eccleston, H.B., Engle, R.E., Govindarajan, S., Satterfield, W., Purcell, R.H., Walker, C.M., Bukh, J., 2010. Novel infectious cDNA clones of hepatitis C virus genotype 3a (strain S52) and 4a (strain ED43): genetic analyses and in vivo pathogenesis studies. J Virol 84(10), 5277-5293.

Gottwein, J.M., Scheel, T.K., Jensen, T.B., Ghanem, L., Bukh, J., 2011b. Differential efficacy of protease inhibitors against HCV genotypes 2a, 3a, 5a, and 6a NS3/4A protease recombinant viruses. Gastroenterology 141(3), 1067-1079.

Hong, S., Freeberg, M.A., Han, T., Kamath, A., Yao, Y., Fukuda, T., Suzuki, T., Kim, J.K., Inoki, K., 2017. LARP1 functions as a molecular switch for mTORC1-mediated translation of an essential class of mRNAs. Elife 6.

Hopkins, T.G., Mura, M., Al-Ashtal, H.A., Lahr, R.M., Abd-Latip, N., Sweeney, K., Lu, H., Weir, J., El-Bahrawy, M., Steel, J.H., Ghaem-Maghami, S., Aboagye, E.O., Berman, A.J., Blagden, S.P., 2016. The RNA-binding protein LARP1 is a post-transcriptional regulator of survival and tumorigenesis in ovarian cancer. Nucleic acids research 44(3), 1227-1246.

Huang, H., Sun, F., Owen, D.M., Li, W., Chen, Y., Gale, M., Jr., Ye, J., 2007. Hepatitis C virus production by human hepatocytes dependent on assembly and secretion of very low-density lipoproteins. Proceedings of the National Academy of Sciences of the United States of America 104(14), 5848-5853.

Jammart, B., Michelet, M., Pecheur, E.I., Parent, R., Bartosch, B., Zoulim, F., Durantel, D., 2013. VLDL-producing and HCV-replicating HepG2 cells secrete no more LVP than VLDL-deficient Huh7.5 cells. J Virol.

Keck, Z.Y., Li, T.K., Xia, J., Bartosch, B., Cosset, F.L., Dubuisson, J., Foung, S.K., 2005. Analysis of a highly flexible conformational immunogenic domain a in hepatitis C virus E2. J Virol 79(21), 13199-13208.

Lahr, R.M., Fonseca, B.D., Ciotti, G.E., Al-Ashtal, H.A., Jia, J.J., Niklaus, M.R., Blagden, S.P., Alain, T., Berman, A.J., 2017. La-related protein 1 (LARP1) binds the mRNA cap, blocking eIF4F assembly on TOP mRNAs. Elife 6.

Lavie, M., Dubuisson, J., 2017. Interplay between hepatitis C virus and lipid metabolism during virus entry and assembly. Biochimie 141, 62-69.

Lindenbach, B.D., 2009. Measuring HCV infectivity produced in cell culture and in vivo. Methods in molecular biology 510, 329-336.

Merret, R., Descombin, J., Juan, Y.T., Favory, J.J., Carpentier, M.C., Chaparro, C., Charng, Y.Y., Deragon, J.M., Bousquet-Antonelli, C., 2013. XRN4 and LARP1 are required for a heat-triggered mRNA decay pathway involved in plant acclimation and survival during thermal stress. Cell Rep 5(5), 1279-1293.

Meunier, J.C., Russell, R.S., Engle, R.E., Faulk, K.N., Purcell, R.H., Emerson, S.U., 2008. Apolipoprotein c1 association with hepatitis C virus. J Virol 82(19), 9647-9656.

Meyer, K., Ait-Goughoulte, M., Keck, Z.Y., Foung, S., Ray, R., 2008. Antibody-dependent enhancement of hepatitis C virus infection. J Virol 82(5), 2140-2149.

Miyanari, Y., Atsuzawa, K., Usuda, N., Watashi, K., Hishiki, T., Zayas, M., Bartenschlager, R., Wakita, T., Hijikata, M., Shimotohno, K., 2007. The lipid droplet is an important organelle for hepatitis C virus production. Nat Cell Biol 9(9), 1089-1097.

Mura, M., Hopkins, T.G., Michael, T., Abd-Latip, N., Weir, J., Aboagye, E., Mauri, F., Jameson, C., Sturge, J., Gabra, H., Bushell, M., Willis, A.E., Curry, E., Blagden, S.P., 2015. LARP1 post-transcriptionally regulates mTOR and contributes to cancer progression. Oncogene 34(39), 5025-5036.

Nickel, W., Rabouille, C., 2009. Mechanisms of regulated unconventional protein secretion. Nat Rev Mol Cell Biol 10(2), 148-155.

Nickel, W., Seedorf, M., 2008. Unconventional mechanisms of protein transport to the cell surface of eukaryotic cells. Annu Rev Cell Dev Biol 24, 287-308.

Parent, R., Qu, X., Petit, M.A., Beretta, L., 2009. The heat shock cognate protein 70 is associated with hepatitis C virus particles and modulates virus infectivity. Hepatology 49(6), 1798-1809.

Patel, M.R., Emerman, M., Malik, H.S., 2011. Paleovirology - ghosts and gifts of viruses past. Curr Opin Virol 1(4), 304-309.

Petersen, T.N., Brunak, S., von Heijne, G., Nielsen, H., 2011. SignalP 4.0: discriminating signal peptides from transmembrane regions. Nature methods 8(10), 785-786.

Piver, E., Boyer, A., Gaillard, J., Bull, A., Beaumont, E., Roingeard, P., Meunier, J.C., 2017. Ultrastructural organisation of HCV from the bloodstream of infected patients revealed by electron microscopy after specific immunocapture. Gut 66(8), 1487-1495.

Reid, A.E., Koziel, M.J., Aiza, I., Jeffers, L., Reddy, R., Schiff, E., Lau, J.Y., Dienstag, J.L., Liang, T.J., 1999. Hepatitis C virus genotypes and viremia and hepatocellular carcinoma in the United States. Am J Gastroenterol 94(6), 1619-1626.

Repetto, G., del Peso, A., Zurita, J.L., 2008. Neutral red uptake assay for the estimation of cell viability/cytotoxicity. Nat Protoc 3(7), 1125-1131.

Stavraka, C., Blagden, S., 2015. The La-Related Proteins, a Family with Connections to Cancer. Biomolecules 5(4), 2701-2722.

Suzuki, Y., Chin, W.X., Han, Q., Ichiyama, K., Lee, C.H., Eyo, Z.W., Ebina, H., Takahashi, H., Takahashi, C., Tan, B.H., Hishiki, T., Ohba, K., Matsuyama, T., Koyanagi, Y., Tan, Y.J., Sawasaki, T., Chu, J.J., Vasudevan, S.G., Sano, K., Yamamoto, N., 2016. Characterization of RyDEN (C19orf66) as an Interferon-Stimulated Cellular Inhibitor against Dengue Virus Replication. PLoS pathogens 12(1), e1005357.

Vichai, V., Kirtikara, K., 2006. Sulforhodamine B colorimetric assay for cytotoxicity screening. Nat Protoc 1(3), 1112-1116.

Xie, C., Huang, L., Xie, S., Xie, D., Zhang, G., Wang, P., Peng, L., Gao, Z., 2013. LARP1 predict the prognosis for early-stage and AFP-normal hepatocellular carcinoma. Journal of translational medicine 11, 272.

Yanagi, M., Purcell, R.H., Emerson, S.U., Bukh, J., 1997. Transcripts from a single full-length cDNA clone of hepatitis C virus are infectious when directly transfected

into the liver of a chimpanzee. Proceedings of the National Academy of Sciences of the United States of America 94(16), 8738-8743.

Fig. 1

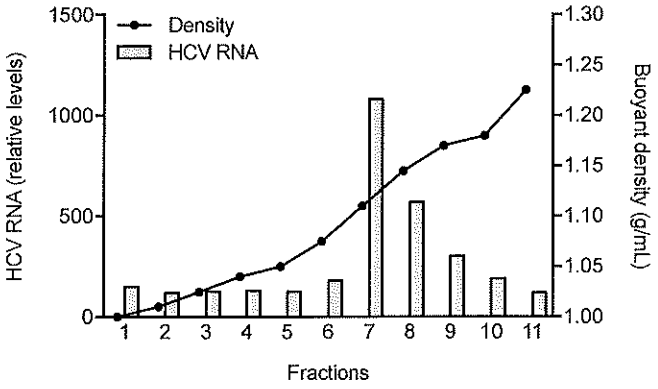
Density
HCV RNA
HCV RNA (relative levels)
Buoyant density (g/mL)
1500
1000
500
0
1.30
1.25
1.20
1.15
1.10
1.05
1.00
1 2 3 4 5 6 7 8 9 10 11
Fractions

Fig. 2

a

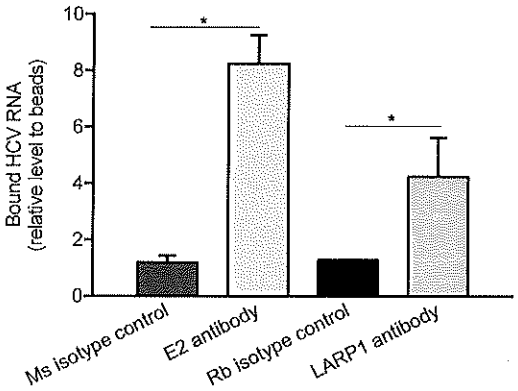
Bound HCV RNA
(relative level to beads)
10
8
6
4
2
0
*
*
Ms isotype control
E2 antibody
Rb isotype control
LARP1 antibody

b

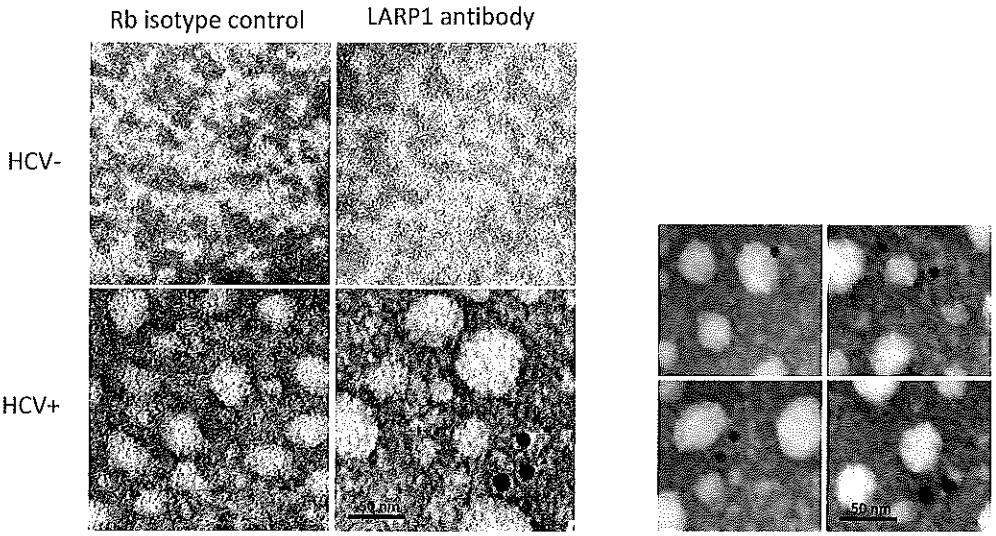
Rb isotype control
LARP1 antibody
HCV-
HCV+
50 nm
50 nm

c

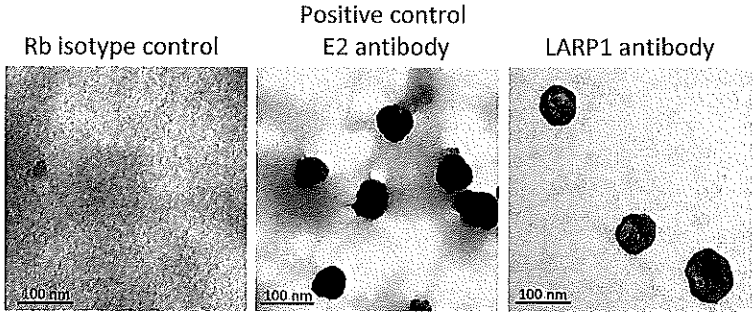
Positive control
Rb isotype control
E2 antibody
LARP1 antibody
100 nm
100 nm
100 nm

Fig. 3

a

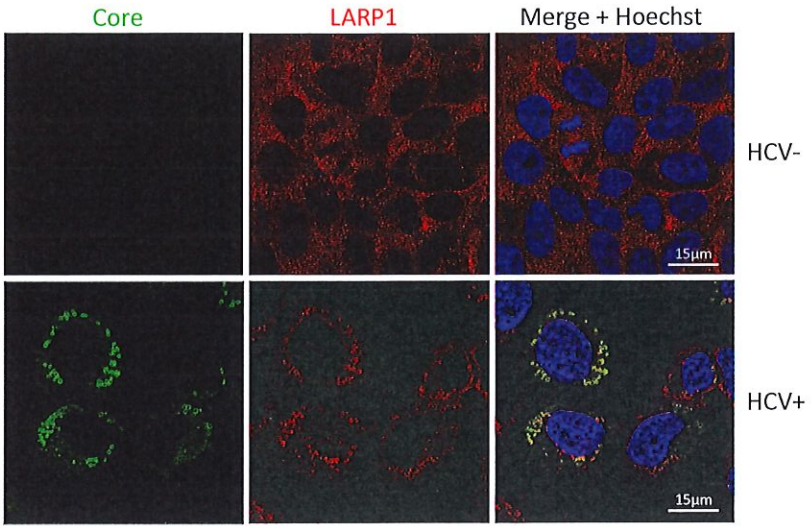
Core
LARP1
Merge + Hoechst
HCV-
HCV+
15µm
15µm

b

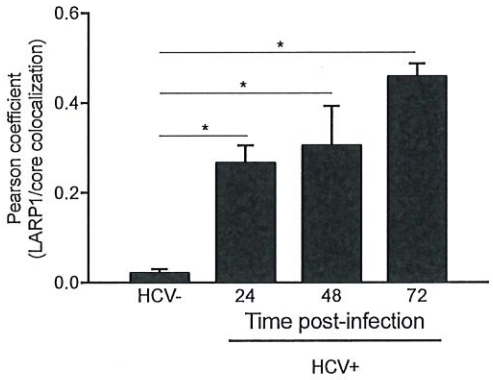
Pearson coefficient
(LARP1/core colocalization)
0.6
0.4
0.2
0.0
*
*
*
HCV-
24
48
72
Time post-infection
HCV+

c

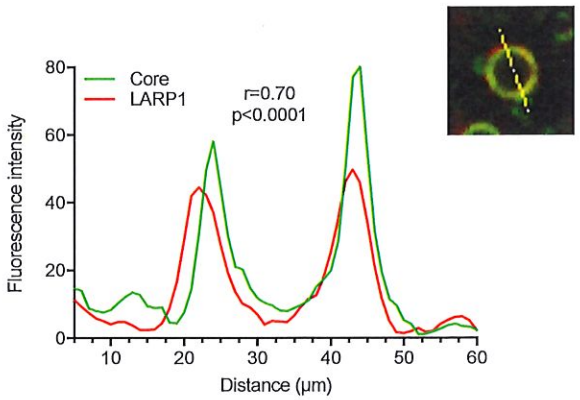
Core
LARP1
r=0.70
p<0.0001
Fluorescence intensity
80
60
40
20
0
10
20
30
40
50
60
Distance (µm)

d

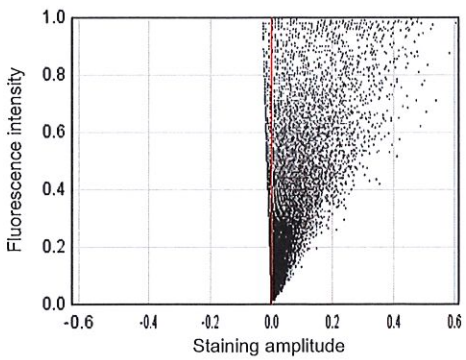
Fluorescence intensity
1.0
0.8
0.6
0.4
0.2
0.0
-0.6
-0.4
-0.2
0.0
0.2
0.4
0.6
Staining amplitude

Fig. 4

a

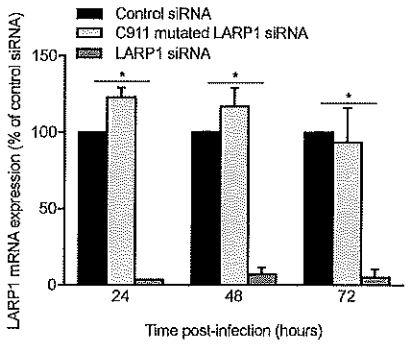
Control siRNA
C911 mutated LARP1 siRNA
LARP1 siRNA
LARP1 mRNA expression (% of control siRNA)
150
100
50
0
*
*
*
24
48
72
Time post-infection (hours)

b

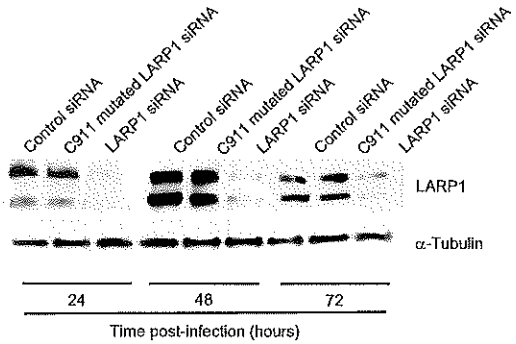
Control siRNA
C911 mutated LARP1 siRNA
LARP1 siRNA
Control siRNA
C911 mutated LARP1 siRNA
LARP1 siRNA
Control siRNA
C911 mutated LARP1 siRNA
LARP1 siRNA
LARP1
α-Tubulin
24
48
72
Time post-infection (hours)

c

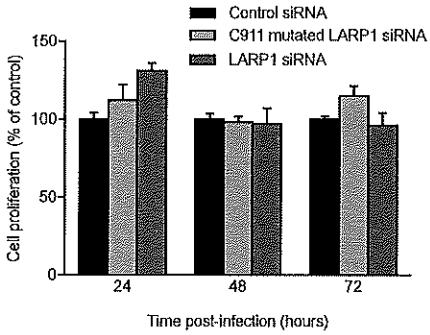
Control siRNA
C911 mutated LARP1 siRNA
LARP1 siRNA
Cell proliferation (% of control)
150
100
50
0
24
48
72
Time post-infection (hours)

d

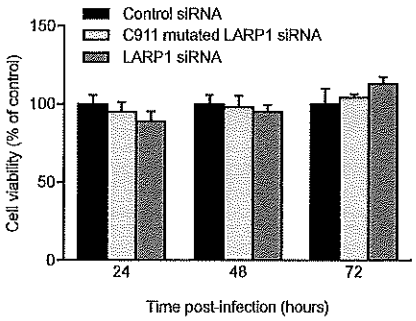
Control siRNA
C911 mutated LARP1 siRNA
LARP1 siRNA
Cell viability (% of control)
150
100
50
0
24
48
72
Time post-infection (hours)

Fig. 5

a

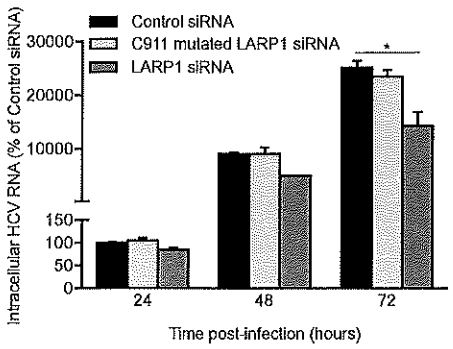

b

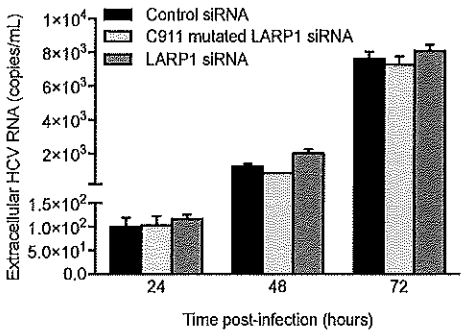

c

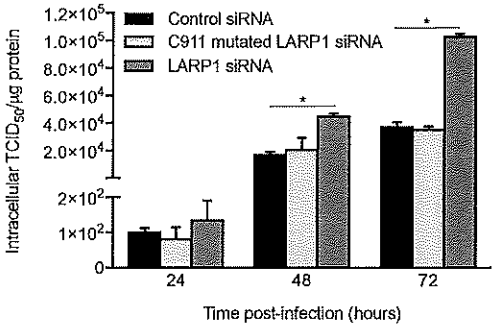

d

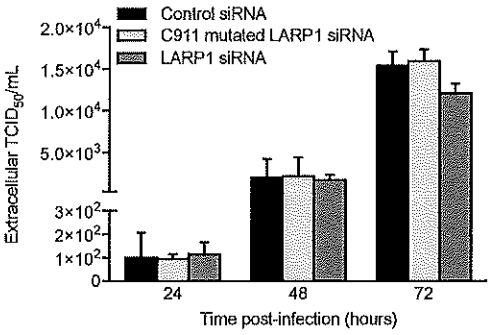

e

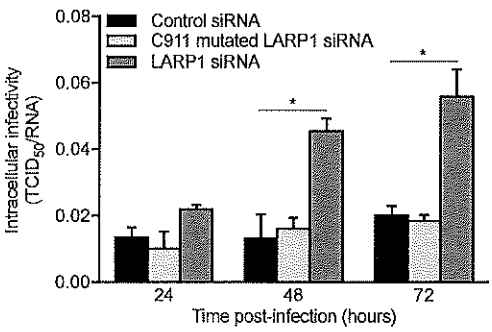

f

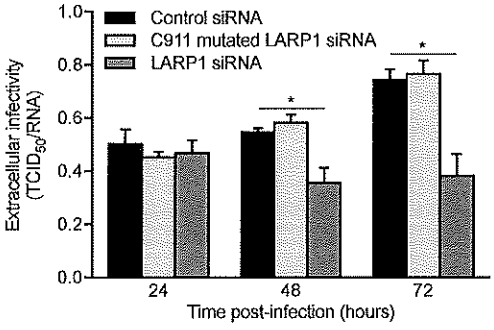

g

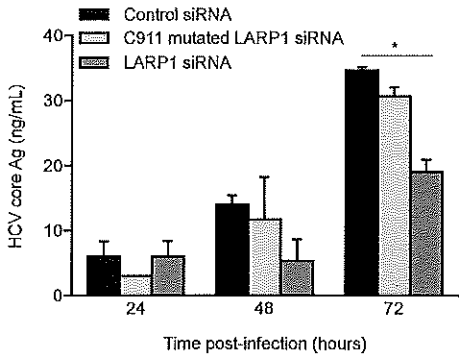

Fig. 6

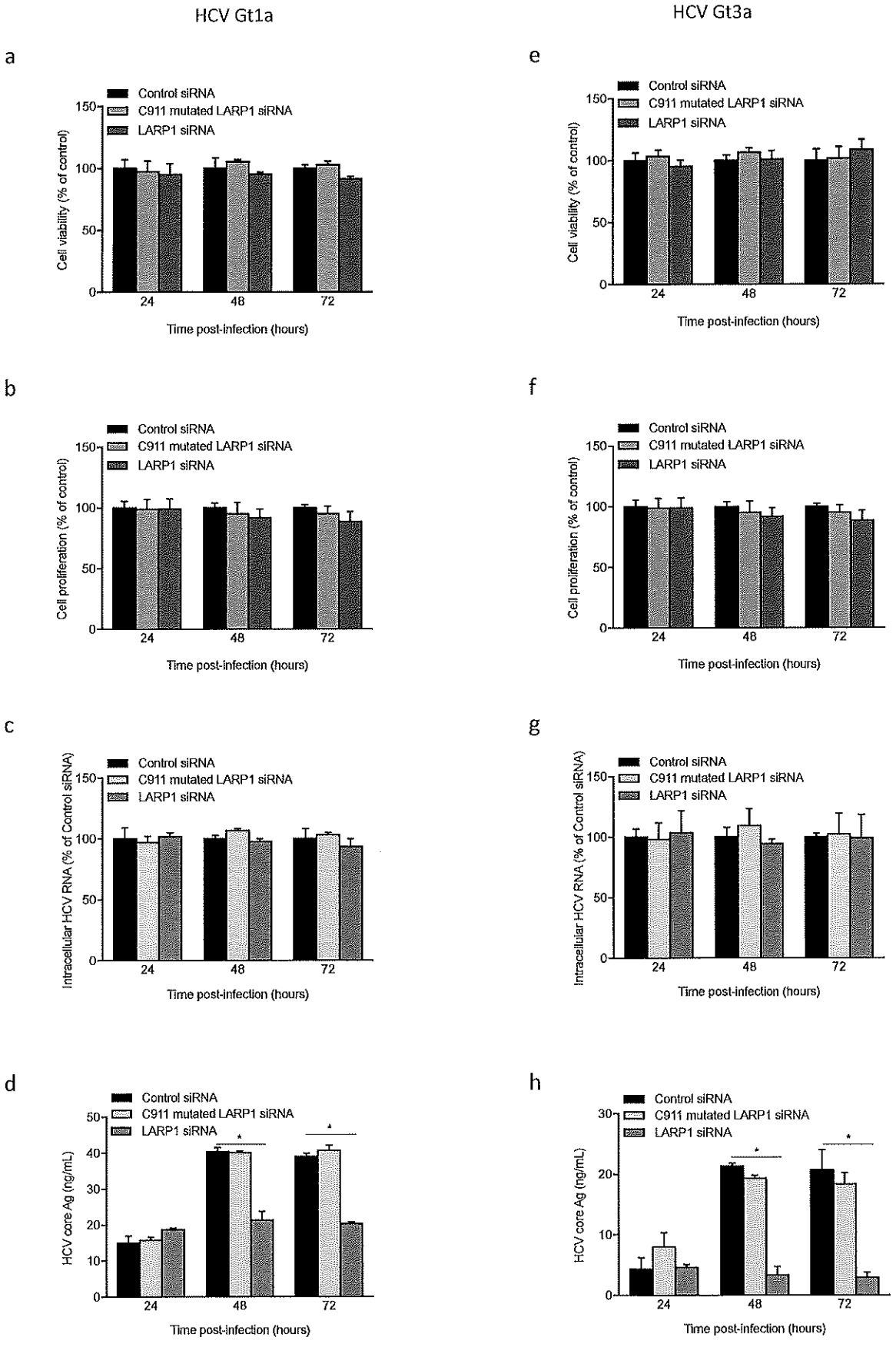
HCV Gt1a
HCV Gt3a
a
e
b
f
c
g
d
h
Control siRNA
C911 mutated LARP1 siRNA
LARP1 siRNA
Cell viability (% of control)
Cell proliferation (% of control)
Intracellular HCV RNA (% of Control siRNA)
HCV core Ag (ng/mL)
Time post-infection (hours)
24
48
72
0
50
100
150
10
20
30
40
*

Supplementary Fig. 1

a

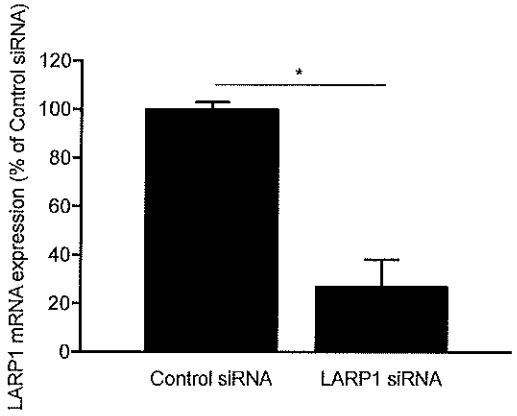

b

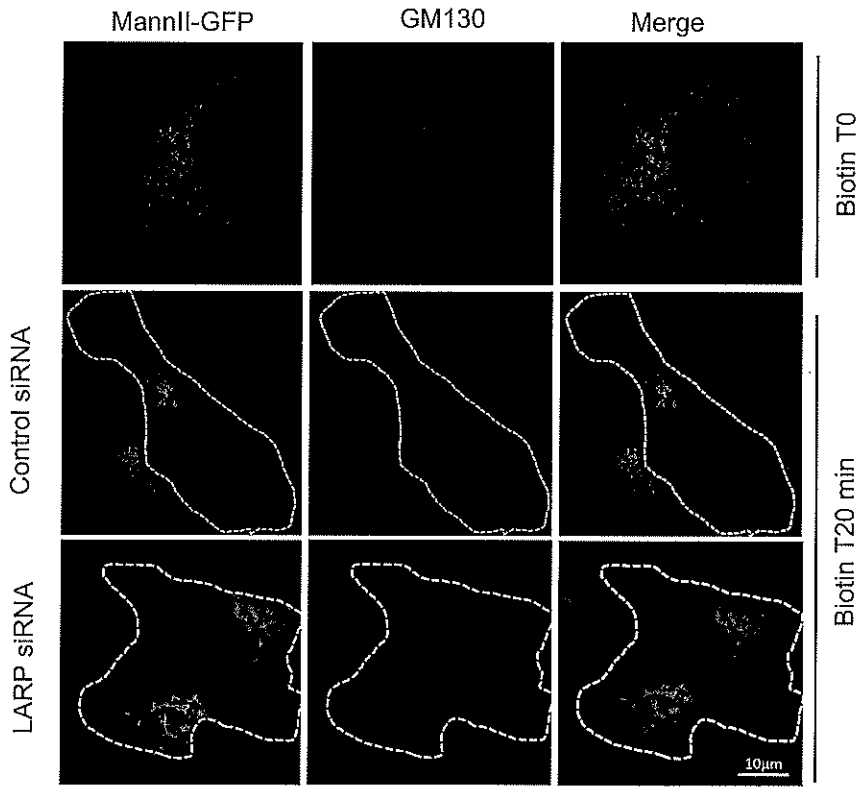

c

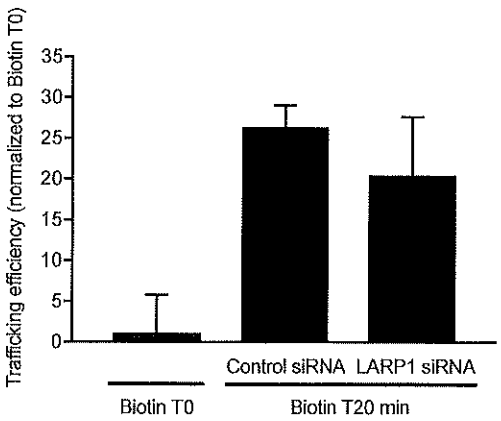

Supplementary Fig. 2